Journal of Functional Foods 84 (2021) 104598

Contents lists available at ScienceDirect

Journal of Functional Foods

journal homepage: www.elsevier.com/locate/jff

Arecanut (*Areca catechu L.*) seed polyphenol improves osteoporosis via gut-serotonin mediated Wnt/β-catenin pathway in ovariectomized rats

Keke Meng [a,b,c,d,1], Fengfeng Mei [a,b,c,d,1], Lehui Zhu [a,c], Qingying Xiang [a,c], Zhangyan Quan [a,c], Feibing Pan [e], Guanghua Xia [a,b,c,d,e,*], Xuanri Shen [a,b,c,d,*], Yonghuan Yun [a,b,c,d], Chenghui Zhang [a,b,c,d], Qiuping Zhong [a,b,c,d], Haiming Chen [a,b,c,d,e]

[a] *Hainan Engineering Research Center of Aquatic Resources Efficient Utilization in South China Sea, Hainan University, Hainan 570228, China*
[b] *Key Laboratory of Food Nutrition and Functional Food of Hainan Province, Haikou 570228, China*
[c] *Engineering Research Center of Utilization of Tropical Polysaccharide Resources, Ministry of Education, Haikou 570228, China*
[d] *College of Food Science and Technology, Hainan University, Hainan 570228, China*
[e] *Huachuang Institute of Areca Research-Hainan, Hainan 570228, China*

ARTICLE INFO

Keywords:
Arecanut (*Areca catechu L.*) seed polyphenol
Serotonin
Serum metabolic
Osteoporosis
Bone formation

ABSTRACT

Arecanut (*Areca catechu L.*) is one of the most important industrial crops in tropical Asia and parts of east Africa. However, the arecanut industry has suffered pandemic loss caused by negative reports such as carcinogenic effect. The healthy development of arecanut industry is of great significance. Our previous study found that arecanut (*Areca catechu L.*) seed polyphenol (ACP) can increase bone mass in ovariectomized rats which is closely related to metabolism of tryptophan. Here, we investigated the relationship among ACP, bone metabolism and serum metabolism in ovariectomized osteoporosis rat. We observed the bone structure of femur and analyzed the LDL-receptor relater protein 5 (LRP5), 5-hydroxytryptophan initial synthetase enzyme 1 (Tph1) and gut-derived serotonin (5-HT) in the gut, bone alkaline phosphatase (BALP), osteocalcin (OCN), Runt-related transcription factor 2 (RUNX2), osteoprotegerin (OPG) and receptor activator of nuclear factor NF-κB ligand (RANKL) in serum, 5-hydroxytryptophan receptor protein (Htr1b), bone morphogenetic protein-2 (BMP2) and β-catenin expression in bone and serum metabolites. The results indicated that compared with osteoporosis rats, ACP significantly improved the damaged bone structure, increased the ratio of OPG/RANKL, Lrp5, BMP2 and β-catenin. The ACP and E2 remarkably enhanced the expression of the metabolites such as 7-Ketodeoxycholic acid, indole and 15-Deoxy-Δ12, 14-prostaglandin, which were deeply linked with 5-HT synthesis via Lrp5 and tryptophan metabolism. Altogether, these studies shown that the ACP could downregulate 5-HT, which were implicated in serum metabolism and promoted bone mass by controlling the bone resorption and formation.

1. Introduction

Osteoporosis is a metabolic disease caused by the failure to set off dynamic bone metabolism balance due to the lopsided bone resorption (Yao et al., 2020). At menopause, estrogen withdrawal altered the bone metabolism, inducing bone loss, and accompanied by altering in the microarchitecture, resulting in bone fragility (Li, Chen, Lu, & Yu, 2020). However, the estrogen analogues as the curative for osteoporosis are limited by the potential adverse effects. The main issue in the treatment of osteoporosis is to identify safe agents which can enhance bone formation and decrease bone resorption caused by menopause on a long-term basis. Thus, there is urgent necessity to identity safe and effectively anti-osteoporosis agents.

Natural products, which plays a key role in regulating osteoimmunological action, can promote bone mass (Hou et al., 2018; Langsetmo, Shikany, & Rogers-Soeder, 2021) by improving bone formation and

Abbreviations: ACP, Arecanut (*Areca catechu L.*) seed polyphenol; BALP, Bone alkaline phosphatase; BMP2, bone morphogenetic protein-2; E2, Estradiol; Htr1b, 5-hydroxytryptophan receptor protein; LRP5, LDL-receptor relater protein5; OCN, Osteocalcin; OPG, Osteoprotegerin; RUNX2, Runt-related transcription factor 2; RANKL, Receptor activator of nuclear factor NF-κB ligand; Tph1, 5-hydroxytryptophan initial synthetase enzyme 1; 5-HT, Serotonin.

* Corresponding authors at: College of Food Science and Technology, Hainan University, Hainan 570228, China.
E-mail addresses: xiaguanghua2011@126.com (G. Xia), shenxuanri2009@163.com (X. Shen).

[1] These authors contributed equally to this study.

https://doi.org/10.1016/j.jff.2021.104598
Received 25 February 2021; Received in revised form 13 June 2021; Accepted 20 June 2021
Available online 22 June 2021

decreasing bone resorption via altering the body's metabolism (Ma et al., 2013; Paccou, 2020). Some international organizations recommend nutritional factors to reduce the risk of osteoporosis (Đudarić, Fužinac-Smojver, Muhvić, & Giacometti, 2015). Natural polyphenolic which presents in various plants and fruits (Hou, Zhang, & Yang, 2019) have been found beneficial to bone health by proinflammatory signaling and modulating osteoimmunological action (Đudarić et al., 2015).

Arecanut (*Areca catechu L.*) is a tropical tree species and is one of the most important industrial crops in tropical Asia and parts of east Africa. In China, the arecanut industry keeps fast developing in the last few years, and has become the pillar industry in Hainan Province (Li et al., 2020). Some evidence confirmed that the chewing of Arecanut might lead to some diseases, such as Type 2 diabetes, oesophageal and oral cancers (Kim et al., 2018; Zhong et al., 2020), which caused a pandemic loss in the arecanut industry. However, as traditional Chinese medicine, Arecanut can be sued to treat parasitic diseases, dyspepsia, edematous and gastrointestinal (Peng et al., 2015). Furthermore, Arecanut extracts have been confirmed to have multiple pharmacological activities, including anti-inflammatory, anti-depressive, antiparasitic effects, and analgesic, as well as other diseases (Bhandare, Kshirsagar, Vyawahare, Hadambar, & Thorve, 2010). Our previous study found that arecanut (*Areca catechu*) seed polyphenols (ACP) exhibited anti-osteoporosis activity (Mei et al., 2021). However, the anti-osteoporosis mechanism and effect of ACP on the metabolites in osteoporotic rats remains unclear.

The gut-derived serotonin (5-hydroxytryptophan, 5-HT) is produced by hydroxylation of tryptophan after decarboxylation and the controlled by 5-hydroxytryptophan initial synthetase enzyme 1 (Tph1) (Yadav et al., 2008; Yano et al., 2015). One of the most popular studied regulators of bone health is LDL-receptor relater protein5 (LRP5) (Yadav et al., 2008)which can be activated by gut and inhibit the synthesis of 5-HT. This interest terms from the founding that the LRP5-deficient mice with decreased 5-HT normalized bone formation and bone mass compared with the ovariectomized WT mice (Yadav et al., 2008). The LRP5 could inhibit expression of Tph1 and the 5-HT act on osteoblasts via the 5-hydroxytryptophan receptor protein (Htr1b) (Boudin et al., 2013) and cAMP response element-binding protein (CREB) (Yang et al., 2020) to inhibit the osteoblasts proliferation (Ducy & Karsenty, 2010). The influence of 5-HT on bone biology can be harnessed pharmacologically to treat osteoporosis. Thus, understanding the 5-HT synthesis metabolism is necessary and urgent.

Based on the emerging link between the 5-HT and osteoblasts, we administrated the ovariectomized rat with ACP for 90 days and used the liquid chromatography coupled with mass spectrometry (LC-MS/MS) as an "omics" tool (Miyamoto et al., 2018; Xu, Pandya, Chung, McClements, & Kinchla, 2018; M. Zhang et al., 2018) to identify specific metabolites involved in 5-HT metabolism. We also investigated bone formation via the serum expression of bone alkaline phosphatase (BALP), osteocalcin (OCN), Runt-related transcription factor 2 (RUNX2), Osteoprotegerin (OPG), and receptor activator of nuclear factor (NF)-κB ligand (RANKL). After that, we further evaluated bone formation by observing the expression of a key protein in the Wnt/β-catenin signal pathway. Our main discovery shown that the ACP could promote bone mass by downregulating 5-HT related to tryptophan metabolism, and the ACP would be a better choice as the therapeutic than E2 associated with the harmful metabolites.

2. Materia and method

2.1. ACP preparation

The Arecanut (*Areca catechu L.*) seed was obtained by Huachuang Institute of areca research-Hainan (Hainan, China). The arecanut seed was ground into a fine powder and passed through a 100-mesh sieve. The powder was soaked in distilled water (w/v = 1:5) at 98 °C for 2 h. The solutions were filtered using a vacuum suction filter (Beijing Holves Biotech Co., Ltd., Beijing, China). After that, for precipitating polysaccharide, the filtrate was mixed with ethyl alcohol (v/v = 1:3) at 4 °C for 12 h. Finally, the sediment was lyophilized by a freeze dryer 126 (Beijing Songyuan Huaxing Bio-Tech Co., Ltd., Beijing, China.), and the ACP was obtained. The main composition of polyphenol was determined using an ultrahigh-performance liquid chromatograph-Xevo triple quadrupole mass spectrometer (UHPLC-MS) with a Waters ACQUITY UPLC BEH C18 (2.1 × 150 mm) column. The compounds were separated by varying the composition of the mobile phase from 95% A (formic acid 0.25 %v/v) and 5% B (formic acid 0.25% v/v in acetonitrile 0.25% v/v) (elution procedure: 0–8 min, 95% A, 8 min, 75% A, 11 min, 40% A, 13 min, 0% A and finally returning to the initial condition at 19 min). The main compositions of ACP are Proanthocyanidin b2, Quinic acid, Procyanidin b1, Catechin, Guaiaverin, trans-/ *cis*-piceid, Naringenin + Naringenin chalcone, trans-/*cis*-resveratrol, leucocyanidin, Syringic acid (Figure S2, Table S1) (Wu, Li, Chen, Wang, & Lin, 2020; Zhu, Zhang, Li, Liu, & Wang, 2020).

2.2. Animals and experimental procedures

All the procedures were dealt with the guidelines of the principle of f Laboratory Animal Care of China Animal Health and Epidemiology Center (www.cahec.cn). A total of 32 female Wister rat (180–200 g) were purchased from TianQin Biotechnology Company of Changsha with Licensed ID: SCXK2014-011 (Changsha, China). The ethical committee of experimental animal care of Hainan university had approved the animal experiments. Rats were raised in the same condition maintained at a constant temperature of 23 °C. The food and water ad libitum were given with a 12 h light–dark cycle (Chen et al., 2018; Mei, Liu, et al., 2020).

After one week of adaptive feeding, the rats were divided into Sham-operated group (n = 8) and ovariectomy group (n = 24) at random. The rats were narcotized by 10% chloral hydrate solution (0.3 mL/100 g. bw). The ovariectomized animals were divided into OVX groups with physiological saline 1 mL/100 g.bw treated, E2 group with E2 drugs 0.3 mg/kg.bw treated and ACP group with ACP (ACP-L, 400 mg/ kg.bw; ACP-H 800 mg/ kg.bw) treated. Meanwhile, the Sham group were intragastric same dose of physiological saline as the OVX group. The rats were received allocated administration once a day on the post-whole experiment.

2.3. Experimental samples collection and Biochemical assay

On the last day of the experiment. All rats were sacrificed. The thighbone, duodenum and liver tissue were dropping into the liquid nitrogen immediately after stripping. The serum was separated by centrifuging (3000 rpm for 20 min at 4 °C). Finally, all the collected materials were stored at −80 °C for analyses.

According to instructions, OCN, BALP, RANKL, and OPG levels in the rat serum were tested using an enzyme-linked immunosorbent assay (ELISA). All kits were purchased from Shanghai MLBIO Biotechnology Co. Ltd. (Shanghai, China).

2.4. Histologic and immunohistochemistry evaluation

The bone tissue was immediately taken into 10% buffered formalin for 24 h after decalcification. Paraffine sections, 5 5 μm thick, were stained with H&E staining. The duodenum was handled the same as the bone tissue and used in immunohistochemical analysis with specific antibodies (5-HT and Tph1). The liver tissue was stained with Oil red staining after the preliminary operation. Then, the pathological section studied with a NIKON Eclipse CiDAP EX340-380 microscope 1 (NIKON, Tokyo, Japan) at a 50× or 400× magnification to evaluate histopanethological situation. All the primary antibodies were purchased from Bioss Biotechnology Co. Ltd. (Beijing, China).

2.5. RNA preparation and qRT-PCR

The total RNA of bone and gut tissue was extracted using Tiangen Animal total RNA extraction kit purchased from Tiangen Biochemical Technology Co., LTD (Beijing, China). All operations followed the manufacturer's instructions. RNA was used to synthesize cDNA with a Reverse transcription first chain synthesise kit (Tiangen Biochemical Technology Co., LTD, Beijing, China). Gene expression levels were investigated by quantitative real-time RT-PCR with the SYBR Green PCR kit (Tiangen Biochemical Technology Co., LTD, Beijing, China) and the 20 uL system using 100 ng of the first-strand cDNA with the following conditions: 95 °C for 15 min followed by 40 cycles at 95 °C for 10 s, 64 °C for 30 s. The primer sets used to amplify target genes are listed in Table 2 (Gu et al., 2021; Mei, Duan, et al., 2020).

2.6. Protein extraction and western blotting

The bone tissue was washed three times with phosphate-buffered saline at 4 °C. After that, the bone was disrupted in an automatic sample grinding machine (Shanghai Jingxin Co., LTD, Shanghai, China). The bone was then extracted with lysis buffer. The total bone lysates were centrifugated at 10,000 rpm for 10 min. Equal amounts of bone lysates were resolved by sodium dodecyl sulfate–polyacrylamide gel electrophoresis on Bio-rad Gel electrophoresis apparatus (American Bio-rad Company, USA), transferred to a PVDF membrane. After that, the membrane was immunoblotted with specific antibodies. Primary antibodies including BMP2, WNT-10β, Smad4, Lrp5, β-catenin and β-actin were purchased from Abcam ((Cambridge, MA, USA). The enhanced chemiluminescence machine with Image Quant LAS4000mini system (General Electric Medical Co. LTD, USA) was used to detect the target proteins, and the quantitative was analyzed with Image J software.

2.7. Serum metabolites extraction

The serum samples moved to −20 °C for 24 h, and then thawed at 4 °C for 12 h. The 100 μL serum was placed in an EP tube, and a 500 L formic solution containing 0.1% formic acid was added, which was then vortex and placed in an ice bath for 5 min. The solution was centrifuged at 5433*g* and 4 °C for 10 min. A certain amount of supernatant was taken and diluted to 53% formic and centrifuged at 5433*g* and 4 °C for 10 min. The supernatant was collected and injected with LC-MS for analysis.

2.8. LC-MS/MS analysis

The LC-MS/MS analysis was completed by the Food College of Hainan University (Hainan, China) and Beijing Nohe Zhiyuan Co., LTD (Beijing, China). The separation was achieved on the Hypesil Gold column (C18) column. The injection volume for each sample was 10 μl. The flow rate was 0.2 mL/min, and the mobile phase consisted of solvent A (0.1% formic and solvent B (100% methanol). The scanning range is m/Z 70–1050; The ESI source is set as follows: Spray Voltage: 3.2 kV; Sheath gas flow rate:40arb; Aux Gas flow rate:10arb; Electro: 320 °C. Electrical: Positive; Negative; MS/MS secondary scans are data-dependent scans.

2.9. Metabolites data analysis

The original data was preprocessed by CD 3.1 data processing software. Firstly, through simple screening of retention time, mass/charge ratio and other parameters, peak alignment was carried out for different samples according to retention time deviation and mass deviation to make identification more accurate. Then the peak was extracted according to the set PPM, signal-to-noise ratio, additive ion and other information, and the peak area was quantified. Then, the metabolites were identified by comparing the high resolution secondary spectrogram databases MZCloud and MZVault and the MassList primary database. Then, metabolites with Coefficient of Variance (CV) less than 30% in QC samples were retained as the final identification result for subsequent analysis. After that, multivariate statistical analysis was performed on the metabolites, including principal component analysis (PCA) and partial least square discriminant analysis (PLS-DA), to reveal the differences in metabolic patterns of different groups.

The screening of differential metabolites mainly referred to VIP, FC and *P*-value three parameters. VIP refers to the variable projection importance of the first principal component of the PLS-DA model, and VIP represents the contribution of metabolites to the grouping. FC refers to the difference multiple, which is the ratio of the mean of repeated quantitative values of each metabolite in all organisms in the comparison group. *P*-value is calculated by *t*-test and represents the significance level of difference. The threshold values were set as VIP > 1.0, FC > 1.5 or FC < 0.667 and P value < 0.05.

After that the heatmap was used to evaluate the the correlation of metabolites. The purpose of differential metabolite correlation analysis is to check the consistency of metabolite and metabolite change trend, and to analyze the correlation between each metabolite by calculating the Pearson correlation coefficient between all the metabolites.

2.10. Statistical analysis

Results Data were expressed as mean ± mean standard error. For all statistical comparisons analysis of different group was using the Anova, LSD and T-test in SPSS software. The statistically significant were accepted with the analysis probability values of P less than 0.05.

3. Results

3.1. ACP ameliorated osteoporosis via improving bone formation

As displayed in Fig. 1, ACP significantly renovated the bone structure compared to the OVX. The losing of bone mass was significantly decreased in ACP compared with OVX. RANKL plays a key role in bone metabolism as a master regulator of bone absorption (Mei et al., 2021). The level of RANKL in serum was remarkably increased after ovariectomy ($P < 0.001$) (Xia et al., 2016), whereas, the ACP treatment could prevent the ovariectomized rats from increasing of RANKL level ($P < 0.001$). To explore the causation between ACP treatment and bone structure outcome, we next assessed the classical osteogenic cytokines serum biochemical indexes of each group, including BALP, OCN, RUNX2 and OPG. Those serum biochemical indexes, including BALP and OPG were significantly increased after ovariectomy ($P < 0.01$) and significantly higher in ACP compared with OVX ($P < 0.001$) (Fig. 1C, G). The value of OPG/RANKL, which was essential for evaluating the bone homeostasis (Tsukasaki et al., 2020), was significantly decreased in OVX and enhanced in ACP and E2 (Fig. 1E), indicating that ACP could increase bone formation in high bone transformation osteoporosis model and improve the bone mass. Interestingly, the content of OCN and RUNX2 were significantly decreased in OVX, and the ACP maintained the normal level of OCN and RUNX2 compared with OVX (Fig. 1F, H). There was no statistical difference between ACP and E2 (Fig. 1C–H). All in all, ACP prevent the loss of bone mass induced by ovariectomy via promoting bone formation. In addition, ACP and positive E2 had the same positive effect on preventing osteoporosis.

3.2. ACP significantly enhanced osteogenesis via the Wnt/β-catenin signaling pathway

Numerous studies have confirmed that the BMP2 plays an important role during bone formation and interacted with the classical pathway of osteogenesis, such as WNT/β-catenin (Chen et al., 2019). To investigate the mechanism of ACP promoting bone formation, we next evaluated the expression of key regulatory factors in WNT/β-catenin by qRT-PCR and western blot. Bone formation related gene expression showed that

Fig. 1. ACP promote bone formation in ovariectomized rat. (A) Experimental procedure schematic. WT rats were treated with ACP (E2 as the Positive drug control group) after ovariectomized. (B) Representative histological image of microstructure bone obtained by H&E staining (n = 7). The contents of bone formation cytokines including OPG (C), RANKNL (D), OPG/RANKL (E), OCN (F), BALP (G) and RUNX2 (H). $^{\#}P < 0.05$ versus Sham, $^{\#\#}P < 0.001$ versus Sham, $^{*}P < 0.05$ versus OVX, $^{**}P < 0.001$ versus OVX.

OVX significantly decreased the expression of WNT-10β, β-catenin and RUNX2 ($P < 0.001$) (Fig. S1). ACP reversed the reduction in these gene expression caused by ovariectomy ($P < 0.001$) (Fig. S1). The gene expression of BMP2 and Smad4 was enhanced after ovariectomy, and the expression in ACP and E2 treated group were significantly higher than that in OVX. Meanwhile, compared to the therapeutic effect of ACP-H, ACP-L showed a stronger activity promoting bone formation gene expression (Fig. S1). As observed by western blot, the result of WNT-10β and β-catenin showed that the femur in ACP expressed higher WNT-10β and β-catenin than in the OVX (Fig. 2A, B and C). BMP2 and Smad4 were strikingly increased in the ACP-treated and E2-treated group. However, both of these proteins were faint in OVX group ($P < 0.01$) (Fig. 2A, D and E). Therefore, these results indicated that ACP could enhance bone formation via WNT/β-catenin.

3.3. ACP induced activation of Lrp5/Tph1/5-HT signaling pathway via up-regulated Lrp5

Previous studies have confirmed that the gut-derived 5-HT is tightly linked to bone formation (Baudry, Schneider, Launay, & Kellermann, 2019; Cui & Kaartinen, 2015). To address the causation and explore the mechanism of osteogenesis. We further assessed the gut expression of Lrp5, which were implicated in 5-HT production (Kode et al., 2014; Yadav et al., 2008). The Lrp5 mRNA expression in ACP was significantly increased than that of OVX ($P < 0.01$). Meanwhile, as observed by western blot, the Lrp5 content of gut in ACP was significantly increased compared to OVX (Fig. 3D, E). The 5-HT production can affect by many factors, but only the Tph1 has been found to have a deep connection with gut-derived 5-HT (Cai et al., 2019; Yu et al., 2019). The Tph1 content increased in the ACP group compared to the OVX group (ACP-OVX, $P < 0.001$; Sham-OVX, $P < 0.001$) (Fig. 3B, F, H). Altered Tph1 contribute to an altered 5-HT expression (Fig. 3G, I). As shown in the immunohistochemical image, the 5-HT was significantly different in the ACP-treated group (ACP-OVX, $P < 0.01$; Sham-OVX, $P < 0.01$). Finally, we detected the mRNA expression of Htr1β, which was known as the 5-HT receptor on osteoblasts. At the genetic level, the Htr1β expression on osteoblasts in the ACP group was significantly decreased than that in the OVX group and even lower than Sham (Fig. 3C) indicated that the osteoblasts in the ACP group had less chance of post exposure to 5-HT. In addition, compared to the therapeutic effect of ACP-H, the ACP-L

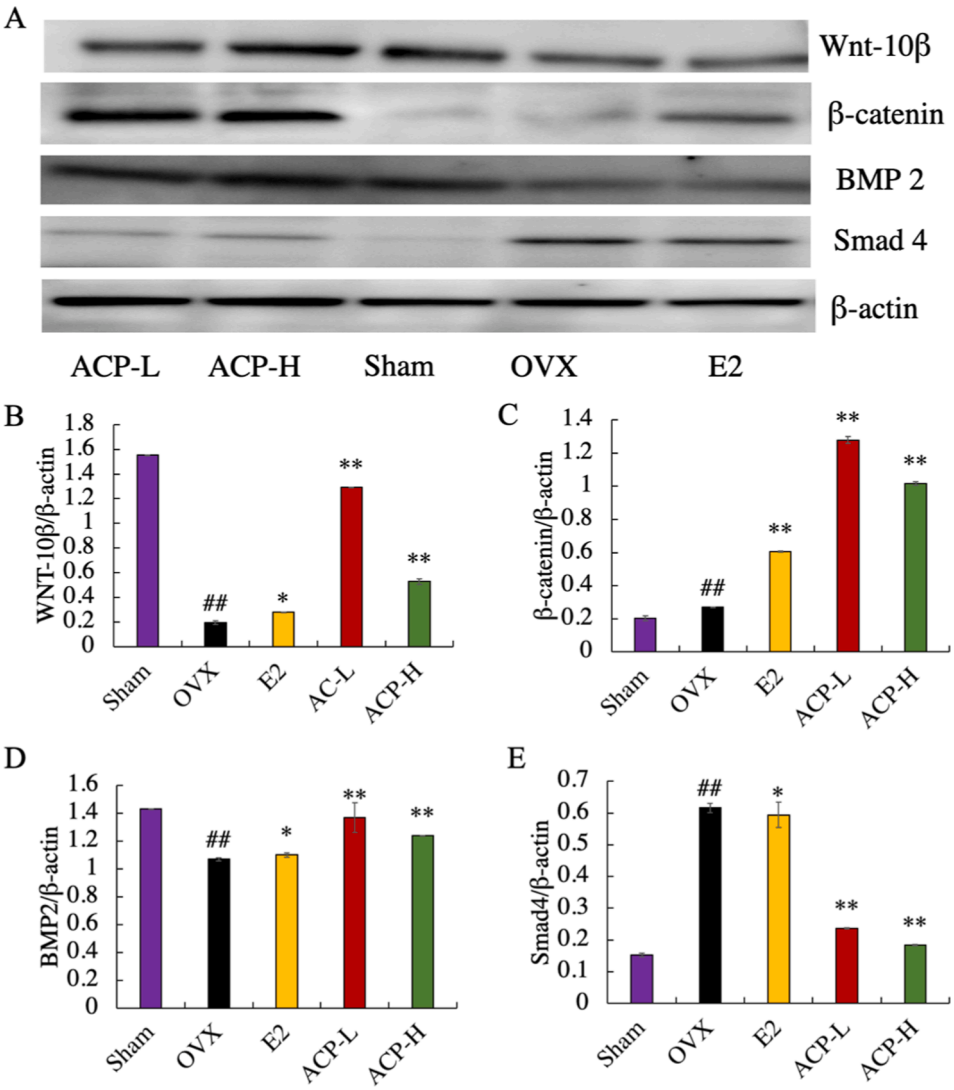

Fig. 2. ACP promote bone formation via WNT/β-catenin pathway. (A) The WNT-10β, BMP2, Smad4 and β-catenin expression of bone was shown with Western blot and (B, C, D, E) the quantified the content of protein was analyzed by Image J. n = 7, $^{\#}P < 0.05$ versus Sham, $^{\#\#}P < 0.001$ versus Sham, $^{*}P < 0.05$ versus OVX, $^{**}P < 0.001$ versus OVX.

showed a stronger activity inhibiting Tph1 and 5-HT and promoting Lrp5 gene expression. These results indicated that the ACP could protect the bone mass by reducing 5-HT via Lrp5/Tph1/5-HT signaling pathway.

3.4. ACP altered liver states and serum metabolism leading to the increasing of Lrp5

To investigate the causation for the change of Lrp5 expression, we further observed the morphology of the liver using oil red and H&E staining. As shown in Fig. 4A, after ovariectomy, hepatoportal vein enlargement was observed in the OVX group, and the reduction of the blue-stained cell nucleus indicated the hepatocyte necrosis was reduced. Oil red-stained fat cell was significantly increased in OVX and significantly decreased after treatment by ACP ($P < 0.001$) revealed that the ACP changed the lipid liver fat anabolism in ovariectomized rat. The H&E staining of the liver showed fatty degeneration of liver cells, necrosis of some liver cells, infiltration of inflammatory cells and haemorrhage in OVX (Fig. 4B). From those pathological analysis, we hypothesis that the ACP could prevent the ovariectomized rats from liver metabolism disorder. In addition, the ACP-L showed a stronger effect to maintain the normal liver function compared to ACP-H.

We next studied the total metabolic diversity serum from Sham, OVX, E2 and ACP-L groups of rats using LC-MS/MS to verify the treatment effect of ACP liver metabolism. The perform multivariate analysis on each group was shown by the PLS-DA model. Principal component analysis profiles (in positive ion model and negative ion mode) at presentation shown clear segregation among metabolic in E2, ACP and OVX (Fig. 4A, B). In the positive ion model, there was a totally of 660 general identification of metabolites of each group in the positive ion model (Table 1). The significant difference in metabolites between Sham and OVX was 88 ($P < 0.05$), including the 41 up-regulated and 47 down-regulated metabolites. The significant difference in metabolites between ACP and OVX was 97 ($P < 0.05$), including the 20 up-regulated and 78 down-regulated metabolites. In the negative ion model, there was a totally of 311 general identification of metabolites of each group, and the significant difference in metabolites between Sham and OVX was 36, including the 28 up-regulated and 8 down-regulated metabolites. The significant difference in metabolites between ACP and OVX was 56 ($P < 0.05$), including the 18 up-regulated and 38 down-regulated metabolites. In addition, the ACP was more readily separated from those of the OVX group in the negative ion model than that in the positive model. These results indicated that the ACP induced an altered serum metabolite in ovariectomized rat via maintaining the normal state of the

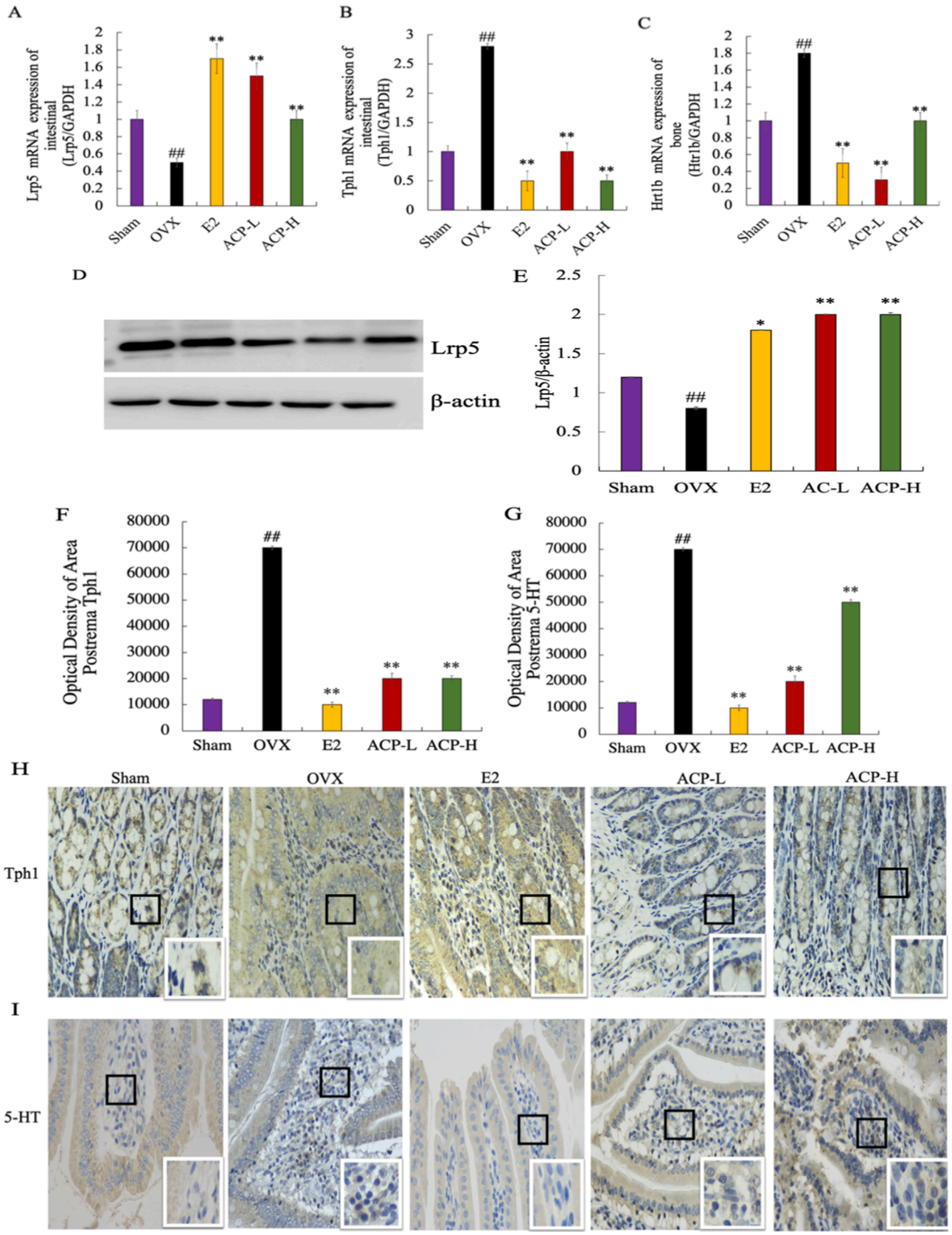

Fig. 3. ACP induces the activation of Lrp5/Tph1/5-HT signaling pathway via regulated Lrp5 and promote bone formation in ovariectomized rats by down-regulated 5-HT. The intestinal Lrp5 (A) and Tph1 (B) mRNA expression of intestinal tract and Htr1β mRNA expression of bone were detected by Q-PCR. The content of intestinal Tph1 (F) and 5-HT (H) were obtained by immumohistochemical staining and observed at 400X. The Optical Density of Tph1 (D) and 5-HT (E) was analyzed by Image Pro plus software. The quanility of Lrp5 was obtained by western blot and analyzed by Image J software. n = 7, $^{\#}P < 0.05$ versus Sham, $^{\#\#}P < 0.001$ versus Sham, $^{*}P < 0.05$ versus OVX, $^{**}P < 0.001$ versus OVX.

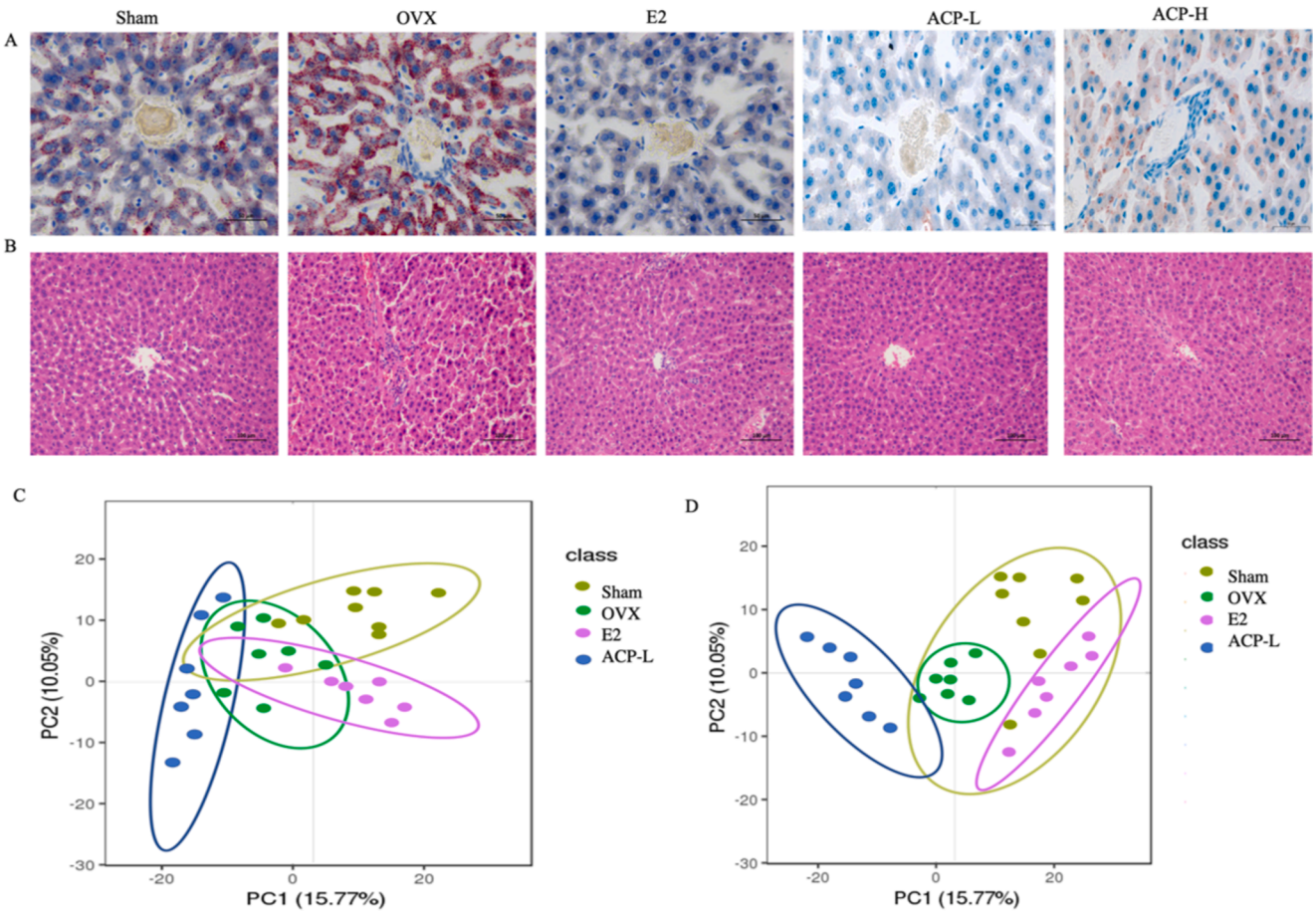

Fig. 4. ACP prevented ovariectomy rats from hepatic steatosis. The lipid content (A) and histological (B) image of liver was observed by Oil red and H&E staining. The serum metabolism of rat was changed by ACP. Score plot of PCA for Sham, OVX, E2 and ACP group in positive ion mode (C) and negative ion mode (D). (For interpretation of the references to colour in this figure legend, the reader is referred to the web version of this article.)

Table 1
Result of metabolite difference screening.

	Compared Samples	Num. of Total Ident.	Num. of Total Sig.	Num. of Sig. Up	Num. of Sig. down
Positive model	OVX.vs. Sham	660	88	41	47
	E2.vs.OVX	660	98	20	78
	ACP.vs.OVX	660	97	37	60
	ACP.vs.E2	660	164	103	61
Negetive model	OVX.vs. Sham	311	36	28	8
	E2.vs.OVX	311	69	11	58
	ACP.vs.OVX	311	56	18	38
	ACP.vs.E2	311	106	71	35

Differential metabolites were screened. *P*-value is calculated by T-test [4], indicating the level of difference significance. The threshold was set as P value < 0.05.
(1) Compared Samples, Compared Samples, Compared Samples.
(2) Num of Total Ident: results of the general identification of metabolites.
(3) Num of Total Sig: the Total number of metabolites with significant differences.
(4) Num of Sig Up: the total number of significantly up-regulated metabolites.
(5) Num of Sig down: the total number of significantly down-regulated metabolites.

Table 2
Primer used for the real-time polymerase chain reaction (Q-PCR).

Gene	Sequence (5′–3′)
Tph1	F-TGCGACATCAACCGAGAACAGC
	R- CGGGCGAGTCCACAGAGAGG
Lrp5	F- CTTCATCCACCGTGCCAACCTG
	R-TCTGCCAGTCTGTCCAGTAGAGTG
Htr1b	F-CACCCTTCTTCTGGCGTCAAGC
	R-CCGTGGAGTAGACCGTGTAGAGG
WNT-10β	F- GTAATCACGACATGGACTTTGGAG
	R- GCACTTCCGCTTCAGGGTTTT
β-catenin	F- CCCGCGAGTACAACCTTCT
	R-CGTCATCCATGGCGAACT
Smad4	F-CAGCCAGGACAGCAGCAGAATG
	R-TGGTGGTGAGGCAAATTAGGTGTG
BMP2	F-AAGCGTCAAGCCAAACACAAACAG
	R- CCAGTCATTCCACCCCACATCAC
GADPH	F-TGCCACTCAGAAGACTGTGG
	R-TTCAGCTCTGGGATGACCTT

liver.

3.5. ACP altered the potential serum metabolic biomarkers of bone loss

To investigate the relationship between potential serum metabolites and bone loss, we further analysed the potential biomarkers by heatmap. The heatmap of the top 20 metabolites was shown in Fig. 5A. The top 4 metabolites, including L-Tryptophan, DL-Tryptophan, PC (16:1e/2:0), Corticosterone, were significantly increased in OVX and ACP-L

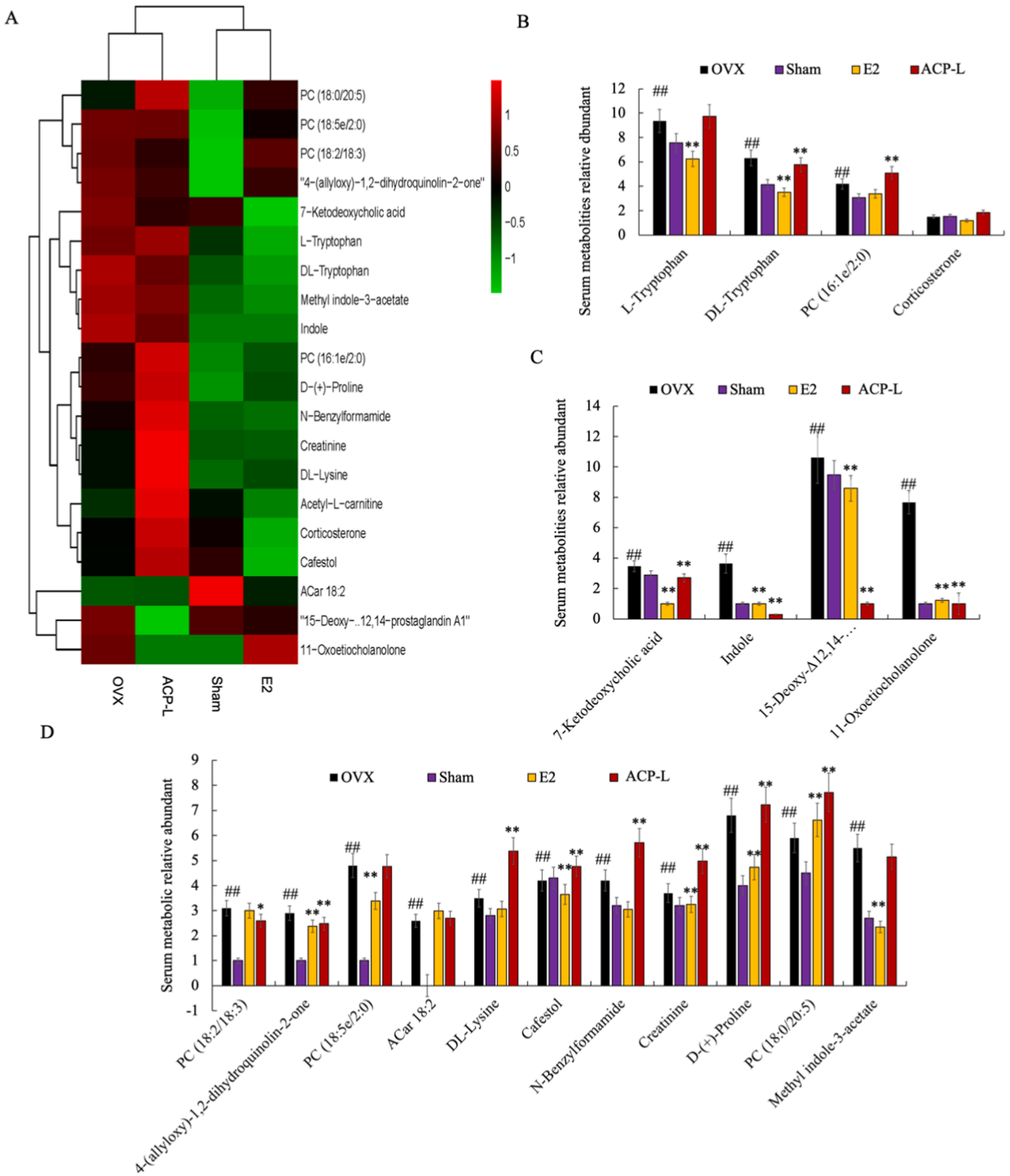

Fig. 5. Heatmap of top 20 differential serum metabolites among OVX, Sham, E2 and ACP-L. Hierarchical clustering analysis was carried out for all the differential metabolites among the obtained comparison pairs, and the relative quantitative values of the differential metabolites were normalized converted and clustered. Vertical is the clustering of samples, horizontal is the clustering of metabolites, the shorter the cluster branches, the higher the similarity. The relationship of the metabolite content clustering among groups can be seen through the horizontal comparison.

compared with Sham and E2 indicated that those four metabolites might be related to estrogen metabolism (Fig. 5A, B). There were 11 metabolites PC (18:2/18:3), 4- (allyloxy)-1,2-dihydroquinolin-2-one, PC (18:5e/2:0), ACar 18:2, DL-Lysine, Cafestol, N-Benzylformamidem, Creatinine, D- (+)-Proline, PC (18:0/20:5), Methyl indole-3-acetate were significantly increased after ovariectomy revealed that those 11 metabolites might be linked with some other function of ovary (Fig. 6A, C). Especially, the 7-Ketodeoxycholic acid, Indole, 15-Deoxy-Δ12,14-prostaglandin A1, 11-Oxoetiocholanolone, which may link with them against bone loss mechanism, were significantly decreased in ACP-L

compared with OVX ($P < 0.01$). Interestingly, 11-Oxoetiocholanolone was significantly increased as OVX after treatment with E2 ($P < 0.01$, E2-Sham). Collectively, these results showed that the ACP significantly altered the main serum metabolites.

4. Discussion

Estrogen deficiency- induced osteoporosis is known as the most common iatrogenic cause of osteoporosis, giving rise to a serious threat to public health (Nik Mohd Hatta et al., 2018; Lizneva et al., 2018). Oral estrogen is an important way to prevent and treat osteoporosis in postmenopausal women (Jiang, Bhandari Randhawa, & Kagan, 2021; Southmayd & De Souza, 2017). However, numbers of studies reported side effects such as nausea, menorrhagia tended to increase for a long-time treatment with estrogen (Coelingh Bennink, Verhoeven, Dutman, & Thijssen, 2017). Therefore, identifying the harmful indicator and searching the safety therapeutic is urgent and important for the prevention of osteoporosis (Iqbal, Yuen, & Zaidi, 2020; Yao et al., 2020). The present study investigated the metabolomics of ovariectomize-induced estrogen deficiency osteoporosis rat and E2 and ACP treatment on serum metabolome. Our study found that the OVX led to up-regulated the expression of Indole, which may be the potential biomarker of bone formation via 5-HT and the expression of Indole was down-regulated after treatment with E2 and ACP.

Bone formation and bone resorption were critical components of bone metabolism. The precise control of bone formation is induced by the osteoblast (Hirose et al., 2020). After ovariectomy, the balance of bone metabolism is disturbed, leading to bone resorption mediated by osteoclast surpassed the bone formation regulated by osteoblast. OPG/RANKL system plays a critical role in the dynamic balance between osteogenesis and bone resorption (Bellido et al., 2010). Here, we observed that the OPG expression was enhanced in the ovariectomized group (OVX, E2 and ACP), and the OPG/RANKL was higher in E2 and ACP than that in OVX based on the ELISA analysis of serum indicated that the ACP could promote bone formation by upregulated the OPG/RANKL ratio. Previous studies found that the expression of OCN would increase when the osteoblasts were active (Lektemur Alpan, Kızıldağ, Özdede, Karakan, & Özmen, 2020). On the contrary, our study found that the OCN was decreased in OVX. It is worth noting that the OCN is secreted by nonproliferating osteoblasts (Fragale et al., 1999; Frediani et al., 2004; Park, Ortinau, Hoggatt, & Scadden, 2021). RUNX2 determines the differentiation of pluripotent stem cells into osteoblasts and can promote osteoblastic maturation (Chen et al., 2020; Ideno et al., 2020). Similarly, in our present study, the expression of RUNX2 was significantly decreased in OVX. Thus, compared with previous studies and our study, we speculated that the immature osteoblasts differentiate actively and mature osteoblasts are few in high bone transformation induced by ovariectomy, and ACP maintained the function of mature osteoblasts. Meanwhile, the OCN is not only a bone formation cytokine, but it is also a cliniopathological marker of the fatty liver hemorrhagic syndrome (Ideno et al., 2020). The liver showed fatty degeneration of liver cells, necrosis of some liver cells, infiltration of inflammatory cells and haemorrhage in OVX and the ACP maintained the normal states of the liver, indicated the pathological changes which may induce the liver metabolic disorder have occurred in the liver of OVX-rats.

Previous studies have declared that the accrual peripheral serotonin is a key inhibitor of bone formation (Cui & Kaartinen, 2015; Ducy & Karsenty, 2010; Yadav et al., 2008). Inflammatory bowel disease patients always have been found the decreasing of bone mass due to the increased 5-HT (Lavoie et al., 2019) indicated that the gut-derived 5-HT influenced (Yano et al., 2015) could inhibit bone formation (Yadav et al., 2010). Lavoie also found that the decreased 5-HT synthesis in DSS-inflamed mice could increase bone mass (Lavoie et al., 2019). Vijay et al. used to an inhibitor of Tph1 which could hamper the biosynthesis of 5-HT as an anabolic mechanism to treat osteoporosis (Yadav et al., 2010). Both two studies revealed that the 5-HT has directly linked to bone formation depending on the expression of Tph1. Similarly, our findings implicated that the ACP and E2 groups with the normal bone mass as Sham compared with OVX ($P < 0.001$) acquired the decreased 5-HT and Tph1 expression. The 5-HT/Htr1b pathway plays a crucial role in the modulation of osteogenesis (Yadav et al., 2008). The 5-HT regulation of osteoblast proliferation was mediated by Htr1b. The 5-HT could inhibit the CREB expression, which could directly affect the osteoblast proliferation, following its binding with Htr1b (Yadav et al., 2008). Our study found that Htr1b, a classical 5-hydroxytryptamine (serotonin) receptor, was significantly decreased after treatment with ACP and E2.

Several reports have shown that the occurred detailed pathway of bone resorption and bone formation can be reflected by metabolites (Xia et al., 2019; Xiao et al., 2018; Zhan et al., 2019). Although the serum metabolism in rat with ovariectomy was altered by E2 and ACP such as PC (18:2/18:3), 4- (allyloxy)-1,2-dihydroquinolin-2-one, PC (18:5e/2:0), ACar 18:2, DL-Lysine, Cafestol, N-Benzylformamidem, Creatinine, D- (+)-Proline, PC (18:0/20:5), Methyl indole-3-acetate, only come special metabolism such as 7-Ketodeoxycholic acid, Indole and 15-Deoxy-Δ12, 14-prostaglandin are related to bone metabolism. We discovered that ACP and E2 treatment could promote bone loss, inducing a complete serum metabolic state compared to the OVX. 7-Ketodeoxycholic acid, Indole and 15-Deoxy-Δ12, 14-prostaglandin A1, were highly decreased in the ACP and E2 compared with OVX ($P < 0.01$). We supposed that the 7-Ketodeoxycholic acid, Indole and 15-Deoxy-Δ12, 14-prostaglandin A1 might be the biomarkers directly linked to bone metabolism. Previous studies showed that the 7-Ketodeoxycholic acid was related to the liver fat metabolism, which might induce the liver injured (Song et al., 2019). The 7-Ketodeoxycholic acid was the final products of cholesterol metabolism in the body (Chen et al., 2016). The 7-Ketodeoxycholic increased in OVX indicated that the cholesterol metabolism induced by the unnormal fat metabolism of the liver. Similar to the previous study, the oil fat staining in our study showed that the fat level was higher in OVX than that in the Sham, ACP and E2 group, which indicated that ovariectomy via altering the fat metabolism to affect bone metabolism. A low bone mineral density correlated with the Lrp5 expression associated with fat accumulation (Loh et al., 2015). Nellie et al. found that the patient with osteoporosis has expressed the highly fat progenitor cells and less Lrp5 and declared that the Lrp5 could regulate the distribution of body fat via a dose-dependent fashion (Loh et al., 2015). Thus, combined with Nellie's finding and our study, we speculated that the fat metabolism of the liver might be regulated via Lrp5 expression. Similarly, the Lrp5 expression at gene level was significantly increased in ACP and E2 compared to OVX ($P < 0.01$) The indole was the final products of tryptophan metabolism (Bartoccini, Fanini, Retini, & Piersanti, 2020). In addition, the 5-HT is known as an indole derivative (Shi et al., 2017) synthesized from tryptophan (Gheorghe et al., 2019) and the main active substance is indoleamine (Carabelli et al., 2020; Maes, Leonard, Myint, Kubera, & Verkerk, 2011). Compared with OVX, the indole and 5-HT expression were significantly decreased in ACP and E2 ($P < 0.001$), indicating that the 5-HT synthesised from tryptophan was inhibited by E2 and ACP. Therefore, we speculate that the ACP and E2 regulated bone mass via tryptophan metabolism, which directly links with the synthesis of 5-HT. However, the serum L-tryptophan and D-tryptophan content were significantly higher in OVX and ACP than in E2 and Sham, suggesting that the content of free tryptophan in serum is related to the expression of estrogen *in vivo*. A previous study also found that the ovariectomy led to a reduction in activity of tryptophan oxygenase in homogenates of the rat liver (Bender, Laing, Vale, Papadaki, & Pugh, 1983). Combined with our studies, we can speculate that the estrogen could improve the synthesis of free L-tryptophan and DL-tryptophan. Collective, the estrogen deficiency induced an increase of tryptophan, the ACP regulated the bone mass via the inhibited production of 5-HT from tryptophan by improved Lrp5.

The 15-Deoxy-$\Delta^{12,14}$-prostaglandin A1 might be the final products of prostaglandin, which released from membranes by phospholipases

(Choudhary & Pilbeam, 2020). With the lower expression in ACP compared with OVX, we inferred that the 15-Deoxy-$\Delta^{12,\ 14}$-prostaglandin A1 was a potential biomarker of bone loss. The 11-Oxoetiocholanolone is a biomarker of glucocorticoid and produced via the glucocorticoid metabolism (Goymann, Mostl, Van't Hof, East, & Hofer, 1999; Ruiz, Eguizábal, Villarreal, Busso, & López, 2019). A long-term increase of glucocorticoid will lead to renal cortical dysfunction, poor sleep and other side effects (Szmyd, Rogut, Białasiewicz, & Gabryelska, 2021). Compared with OVX, the 11-Oxoetiocholanolone was remarkably decreased in ACP and increased in E2, indicated that both the lack of estrogen or long-term oral estrogen could induce the disorder of glucocorticoid metabolism. These results revealed that E2 and ACP both have the anti-osteoporosis effect in ovariectomized rats, but the E2 might induce a lot of side effects via the improved glucocorticoid metabolism.

The bone formation could be cooperatively regulated by BMP2 and Wnt/β-catenin signaling pathway (Zhang et al., 2013; Zhao et al., 2020). In osteoblasts, the wnt/β-catenin signaling pathway could transactivates BMP2 expression via β-catenin/T cell specific factor (TFC)4 by specific TCF binding in the BMP2 promoter (Zhang et al., 2013), leading the bone formation (Miszuk et al., 2018). In addition, BMP2-mediated activation of type I receptors and type II serine/threonine kinase receptors stimulates phosphorylation of Smad1, Smad5, and Smad8, and the subsequent formation of isomer complexes with Smad4 (Gangwen, HanXiao-Jing, & Wang, 2011; Si et al., 2014). Smad4 complexes migrate to the nucleus, where they cooperate with co-activators or co-repressors to regulate gene expression. Smad4 encodes the only common Smad4 protein in mammals and is a key nuclear mediator in the BMP2 signaling pathway. In addition to promoting SMAD4-mediated transcription, BMP2 ligands may also stimulate other molecules through the "atypical" kinase pathway. We hypothesized that the ACP altered the Lrp5/Tph1/5-HT signaling pathway and the down upregulated 5-HT increased the osteoblast leading to the activation of wnt/β-catenin. Western blot showed that the BMP2 and β-catenin results were consistent with the hypothesis, both were higher in ACP than those in OVX ($P < 0.01$).

5. Conclusion

Taken together, this present study revealed that ACP could improve osteoporosis by regulating the expression of 5-HT, which were implicated in the regulation of bone formation. It promoted bone formation by controlling the osteoblasts proliferation via BMP2. However, from metabolism and nutritional perspective, the ACP, which induced the lower 11-Oxoetiocholanolone production, are safer than E2. Understanding the potential biomarkers of bone metabolic mechanism is beneficial to the treatment of osteoporosis. In addition, the indole can be treated as an important biomarker, and the influence of indole metabolism on bone health is worthy of further research.

6. Ethics statements

The study was performed in accordance with the Experimental Animal Administration regulations issued by the State Committee of Science and Technology of the People's Republic of China and the Guidelines for Care and Use of Laboratory Animals of Hainan University. The ethical approval reference number of the study is HNDX2020072. All the procedures for the care of the rats were in accordance with the institutional guidelines for animal use in research.

CRediT authorship contribution statement

Keke Meng: Methodology, Software, Writing - original draft, Project administration, Visualization, Writing - review & editing. **Fengfeng Mei:** Methodology, Software, Writing - original draft, Project administration, Visualization, Writing - review & editing. **Lehui Zhu:** Writing - review & editing. **Qingying Xiang:** Writing - review & editing. **Zhangyan Quan:** Writing - review & editing. **Feibing Pan:** Supervision, Funding acquisition. **Guanghua Xia:** Conceptualization, Investigation, Funding acquisition. **Xuanri Shen:** Conceptualization, Investigation, Funding acquisition. **Yonghuan Yun:** Formal analysis, Investigation. **Chenghui Zhang:** Formal analysis, Investigation. **Qiuping Zhong:** Formal analysis, Investigation. **Haiming Chen:** Supervision, Funding acquisition.

Declaration of Competing Interest

The authors declare that they have no known competing financial interests or personal relationships that could have appeared to influence the work reported in this paper.

Acknowledgements

This work was supported by Primary Research & Development Plan of Hainan Province (no: ZDYF2020224), the Program of Hainan Association for Science and Technology Plans to Youth R&D Innovation (No. QCXM202003), Fund of Dean of Huachuang Institute of Areca Research-Hainan (HD-KYH-2020037, HCBL2020YZ-007), and the Scientific Research Foundation of Hainan University (no. kyqd1662).

Appendix A. Supplementary material

Supplementary data to this article can be found online at https://doi.org/10.1016/j.jff.2021.104598.

References

Bartoccini, F., Fanini, F., Retini, M., & Piersanti, G. (2020). General synthesis of unnatural 4-, 5-, 6-, and 7-bromo-d-tryptophans by means of a regioselective indole alkylation. *Tetrahedron Letters, 61*(22), Article 151923. https://doi.org/10.1016/j.tetlet.2020.151923.

Baudry, A., Schneider, B., Launay, J.-M., & Kellermann, O. (2019). Serotonin in stem cell based-dental repair and bone formation: A review. *Biochimie, 161*, 65–72. https://doi.org/10.1016/j.biochi.2018.07.030.

Bellido, M., Lugo, L., Roman-Blas, J. A., Castaneda, S., Caeiro, J. R., Dapia, S., … Herrero-Beaumont, G. (2010). Subchondral bone microstructural damage by increased remodelling aggravates experimental osteoarthritis preceded by osteoporosis. *Arthritis Research & Therapy, 12*(4). https://doi.org/10.1186/ar3103.

Bender, D. A., Laing, A. E., Vale, J. A., Papadaki, L., & Pugh, M. (1983). The effects of oestrogen administration on tryptophan metabolism in rats and in menopausal women receiving hormone replacement therapy. *Biochemical Pharmacology, 32*(5), 843–848. https://doi.org/10.1016/0006-2952 (83)90586-5.

Bhandare, A. M., Kshirsagar, A. D., Vyawahare, N. S., Hadambar, A. A., & Thorve, V. S. (2010). Potential analgesic, anti-inflammatory and antioxidant activities of hydroalcoholic extract of Areca catechu L. nut. *Food and Chemical Toxicology, 48*(12), 3412–3417. https://doi.org/10.1016/j.fct.2010.09.013.

Boudin, E., Jennes, K., de Freitas, F., Tegay, D., Mortier, G., & Van Hul, W. (2013). No mutations in the serotonin related TPH1 and HTR1B genes in patients with monogenic sclerosing bone disorders. *Bone, 55*(1), 52–56. https://doi.org/10.1016/j.bone.2013.03.015.

Cai, M., Zhou, L., Liao, J., Huang, Q., Xia, Z., & Shang, J. (2019). IFN-γ inhibits 5-HT-induced melanin biosynthesis via downregulation of 5-HT receptors in vivo/in vitro. *Journal of Pharmacological Sciences, 141*(1), 1–8. https://doi.org/10.1016/j.jphs.2019.05.005.

Carabelli, B., Delattre, A. M., Waltrick, A. P. F., Araújo, G., Suchecki, D., Machado, R. B., … Ferraz, A. C. (2020). Fish-oil supplementation decreases Indoleamine-2,3-Dioxygenase expression and increases hippocampal serotonin levels in the LPS depression model. *Behavioural Brain Research, 390*, Article 112675. https://doi.org/10.1016/j.bbr.2020.112675.

Chen, H., Cao, G., Chen, D.-Q., Wang, M., Vaziri, N. D., Zhang, Z.-H., … Zhao, Y.-Y. (2016). Metabolomics insights into activated redox signaling and lipid metabolism dysfunction in chronic kidney disease progression. *Redox Biology, 10*, 168–178. https://doi.org/10.1016/j.redox.2016.09.014.

Chen, S., Jing, J., Yuan, Y., Feng, J., Han, X., Wen, Q., … Chai, Y. (2020). Runx2+ niche cells maintain incisor mesenchymal tissue homeostasis through IGF signaling. *Cell Reports, 32*(6), Article 108007. https://doi.org/10.1016/j.celrep.2020.108007.

Chen, X.-J., Shen, Y.-S., He, M.-C., Yang, F., Yang, P., Pang, F.-X., … Wei, Q.-S. (2019). Polydatin promotes the osteogenic differentiation of human bone mesenchymal stem cells by activating the BMP2-Wnt/β-catenin signaling pathway. *Biomedicine & Pharmacotherapy, 112*, Article 108746. https://doi.org/10.1016/j.biopha.2019.108746.

Chen, Y., Gao, X., Wei, Y., Liu, Q., Jiang, Y., Zhao, L., & Ulaah, S. (2018). Isolation, purification and the anti-hypertensive effect of a novel angiotensin I-converting enzyme (ACE) inhibitory peptide from Ruditapes philippinarum fermented with

Bacillus natto. *Food & Functionions, 9*(10), 5230–5237. https://doi.org/10.1039/c8fo01146j.
Choudhary, S., & Pilbeam, C. (2020). Chapter 51 - Prostaglandins and bone metabolism. In J. P. Bilezikian, T. J. Martin, T. L. Clemens, & C. J. Rosen (Eds.), *Principles of Bone Biology* (4th ed., pp. 1247–1269). Academic Press.
Coelingh Bennink, H. J. T., Verhoeven, C., Dutman, A. E., & Thijssen, J. (2017). The use of high-dose estrogens for the treatment of breast cancer. *Maturitas, 95*, 11–23. https://doi.org/10.1016/j.maturitas.2016.10.010.
Cui, C., & Kaartinen, M. T. (2015). Serotonin (5-HT) inhibits Factor XIII-A-mediated plasma fibronectin matrix assembly and crosslinking in osteoblast cultures via direct competition with transamidation. *Bone, 72*, 43–52. https://doi.org/10.1016/j.bone.2014.11.008.
Ducy, P., & Karsenty, G. (2010). The two faces of serotonin in bone biology. *Journal of Cell Biology, 191*(1), 7–13. https://doi.org/10.1083/jcb.201006123.
Đudarić, L., Fužinac-Smojver, A., Muhvić, D., & Giacometti, J. (2015). The role of polyphenols on bone metabolism in osteoporosis. *Food Research International, 77*, 290–298. https://doi.org/10.1016/j.foodres.2015.10.017.
Fragale, A., Tartaglia, M., Bernardini, S., Di Stasi, A. M. M., Di Rocco, C., Velardi, F., … Migliaccio, S. (1999). Decreased proliferation and altered differentiation in osteoblasts from genetically and clinically distinct craniosynostotic disorders. *The American Journal of Pathology, 154*(5), 1465–1477. https://doi.org/10.1016/S0002-9440 (10)65401-6.
Frediani, B., Spreafico, A., Capperucci, C., Chellini, F., Gambera, D., Ferrata, P., … Marcolongo, R. (2004). Long-term effects of neridronate on human osteoblastic cell cultures. *Bone, 35*(4), 859–869. https://doi.org/10.1016/j.bone.2004.06.001.
Gangwen, HanXiao-Jing, & Wang. (2011). Roles of TGFβ signaling Smads in squamous cell carcinoma. *Cell & Bioscience*.
Gheorghe, C. E., Martin, J. A., Manriquez, F. V., Dinan, T. G., Cryan, J. F., & Clarke, G. (2019). Focus on the essentials: Tryptophan metabolism and the microbiome-gut-brain axis. *Current Opinion in Pharmacology, 48*, 137–145. https://doi.org/10.1016/j.coph.2019.08.004.
Goymann, W., Mostl, E., Van't Hof, T., East, M. L., & Hofer, H. (1999). Noninvasive fecal monitoring of glucocorticoids in spotted hyenas, Crocuta crocuta. *General and Comparative Endocrinology, 114*(3), 340–348. https://doi.org/10.1006/gcen.1999.7268.
Gu, Z., Zhu, Y., Mei, F., Dong, X., Xia, G., & Shen, X. (2021). Tilapia head glycolipids protect mice against dextran sulfate sodium-induced colitis by ameliorating the gut barrier and suppressing NF-kappa B signaling pathway. *International Immunopharmacology, 96*, Article 107802. https://doi.org/10.1016/j.intimp.2021.107802.
Hirose, K., Ishimoto, T., Usami, Y., Sato, S., Oya, K., Nakano, T., … Toyosawa, S. (2020). Overexpression of Fam20C in osteoblast in vivo leads to increased cortical bone formation and osteoclastic bone resorption. *Bone, 138*, Article 115414. https://doi.org/10.1016/j.bone.2020.115414.
Hou, T., Zhang, L., & Yang, X. (2019). Ferulic acid, a natural polyphenol, protects against osteoporosis by activating SIRT1 and NF-κB in neonatal rats with glucocorticoid-induced osteoporosis. *Biomedicine & Pharmacotherapy, 120*, Article 109205. https://doi.org/10.1016/j.biopha.2019.109205.
Hou, Y.-C., Wu, C.-C., Liao, M.-T., Shyu, J.-F., Hung, C.-F., Yen, T.-H., … Lu, K.-C. (2018). Role of nutritional vitamin D in osteoporosis treatment. *Clinica Chimica Acta, 484*, 179–191. https://doi.org/10.1016/j.cca.2018.05.035.
Ideno, H., Nakashima, K., Komatsu, K., Araki, R., Abe, M., Arai, Y., … Nifuji, A. (2020). G9a is involved in the regulation of cranial bone formation through activation of Runx2 function during development. *Bone, 137*, Article 115332. https://doi.org/10.1016/j.bone.2020.115332.
Iqbal, J., Yuen, T., & Zaidi, M. (2020). Getting warmer: Following one's gut to build bone. *Cell Metabolism, 32*(4), 504–506. https://doi.org/10.1016/j.cmet.2020.09.010.
Jiang, X., Bhandari Randhawa, S., & Kagan, R. (2021). Chapter 73 - Estrogen and estrogen analogs for prevention and treatment of osteoporosis. In D. W. Dempster, J. A. Cauley, M. L. Bouxsein & F. Cosman (Eds.), Marcus and Feldman's Osteoporosis (Fifth Edition) (pp. 1711–1719): Content Repository Only!.
Kim, H.-J., Ko, J.-W., Cha, S.-B., Heo, H.-S., Seo, J.-H., Cha, M.-J., … Kim, J.-C. (2018). Evaluation of 13-week repeated oral dose toxicity of Areca catechu in F344/N rats. *Food and Chemical Toxicology, 114*, 41–51. https://doi.org/10.1016/j.fct.2018.02.015.
Kode, A., Obri, A., Paone, R., Kousteni, S., Ducy, P., & Karsenty, G. (2014). Lrp5 regulation of bone mass and serotonin synthesis in the gut. *Nature Medicine, 20*(11), 1228–1229. https://doi.org/10.1038/nm.3698.
Langsetmo, L., Shikany, J. M., & Rogers-Soeder, T. (2021). Chapter 21 - Nutrition and osteoporosis. In D. W. Dempster, J. A. Cauley, M. L. Bouxsein & F. Cosman (Eds.), Marcus and Feldman's Osteoporosis (Fifth Edition) (pp. 503–529): Content Repository Only!.
Lavoie, B., Roberts, J. A., Haag, M. M., Spohn, S. N., Margolis, K. G., Sharkey, K. A., … Mawe, G. M. (2019). Gut-derived serotonin contributes to bone deficits in colitis. *Pharmacological Research, 140*, 75–84. https://doi.org/10.1016/j.phrs.2018.07.018.
Lektemur Alpan, A., Kızıldağ, A., Özdede, M., Karakan, N. C., & Özmen, Ö. (2020). The effects of taxifolin on alveolar bone in experimental periodontitis in rats. *Archives of Oral Biology, 117*, Article 104823. https://doi.org/10.1016/j.archoralbio.2020.104823.
Li, J., Chen, X., Lu, L., & Yu, X. (2020). The relationship between bone marrow adipose tissue and bone metabolism in postmenopausal osteoporosis. *Cytokine & Growth Factor Reviews, 52*, 88–98. https://doi.org/10.1016/j.cytogfr.2020.02.003.
Li, J., Jia, X., Liu, L., Cao, X., Xiong, Y., Yang, Y., … Li, M. (2020). Comparative biochemical and transcriptome analysis provides insights into the regulatory mechanism of striped leaf albinism in arecanut (Areca catechu L.). *Industrial Crops and Products, 154*, Article 112734. https://doi.org/10.1016/j.indcrop.2020.112734.
Lizneva, D., Yuen, T., Sun, L., Kim, S.-M., Atabiekov, I., Munshi, L. B., … Zaidi, M. (2018). Emerging concepts in the epidemiology, pathophysiology, and clinical care of osteoporosis across the menopausal transition. *Matrix Biology, 71–72*, 70–81. https://doi.org/10.1016/j.matbio.2018.05.001.
Loh, Nellie Y., Neville, Matt J., Marinou, K., Hardcastle, Sarah A., Fielding, Barbara A., Duncan, Emma L., … Christodoulides, C. (2015). LRP5 regulates human body fat distribution by modulating adipose progenitor biology in a dose- and depot-specific fashion. *Cell Metabolism, 21*(2), 262–273. https://doi.org/10.1016/j.cmet.2015.01.009.
Ma, B., Li, X., Zhang, Q., Wu, D., Wang, G. A. J., … Ying, H. (2013). Metabonomic profiling in studying anti-osteoporosis effects of strontium fructose 1,6-diphosphate on estrogen deficiency-induced osteoporosis in rats by GC/TOF-MS. *European Journal of Pharmacology, 718*(1–3), 524–532. https://doi.org/10.1016/j.ejphar.2013.06.030.
Maes, M., Leonard, B. E., Myint, A. M., Kubera, M., & Verkerk, R. (2011). The new '5-HT' hypothesis of depression: Cell-mediated immune activation induces indoleamine 2,3-dioxygenase, which leads to lower plasma tryptophan and an increased synthesis of detrimental tryptophan catabolites (TRYCATs), both of which contribute to the onset of depression. *Progress in Neuro-Psychopharmacology and Biological Psychiatry, 35*(3), 702–721. https://doi.org/10.1016/j.pnpbp.2010.12.017.
Mei, F., Duan, Z., Chen, M., Lu, J., Zhao, M., Li, L., … Chen, S. (2020). Effect of a high-collagen peptide diet on the gut microbiota and short-chain fatty acid metabolism. *Journal of Functional Foods, 75*, Article 104278. https://doi.org/10.1016/j.jff.2020.104278.
Mei, F., Liu, J., Wu, J., Duan, Z., Chen, M., Meng, K., … Zhao, M. (2020). Collagen peptides isolated from salmo salar and tilapia nilotica skin accelerate wound healing by altering cutaneous microbiome colonization via upregulated NOD2 and BD14. *Journal of Agricultural and Food Chemistry, 68*(6), 1621–1633. https://doi.org/10.1021/acs.jafc.9b08002.
Mei, F., Meng, K., Gu, Z., Yun, Y., Zhang, W., Zhang, C., … Chen, H. (2021). Arecanut (Areca catechu L.) seed polyphenol-ameliorated osteoporosis by altering gut microbiome via LYZ and the immune system in estrogen-deficient rats. *Journal of Agricultural and Food Chemistry, 69*(1), 246–258. https://doi.org/10.1021/acs.jafc.0c06671.
Miszuk, J. M., Xu, T., Yao, Q., Fang, F., Childs, J. D., Hong, Z., … Sun, H. (2018). Functionalization of PCL-3D electrospun nanofibrous scaffolds for improved BMP2-induced bone formation. *Applied Materials Today, 10*, 194–202. https://doi.org/10.1016/j.apmt.2017.12.004.
Miyamoto, T., Hirayama, A., Sato, Y., Koboyashi, T., Katsuyama, E., Kanagawa, H., … Matsumoto, M. (2018). Metabolomics-based profiles predictive of low bone mass in menopausal women. *Bone Reports, 9*, 11–18. https://doi.org/10.1016/j.bonr.2018.06.004.
Nik Mohd Hatta, N. N. K., Lokman, M., Said, N. M., Daud, A., Ibrahim, M., Sharifudin, M. A., & Deraman, S. (2018). Fracture risk prediction in post-menopausal women with osteopenia and osteoporosis: preliminary findings. *Enfermería Clínica, 28*, 232–235. https://doi.org/10.1016/S1130-8621 (18)30074-3.
Paccou, J. (2020). Nutritional facets of osteoporosis management: Can probiotics help? *Joint Bone Spine, 87*(2), 115–117. https://doi.org/10.1016/j.jbspin.2019.06.007.
Park, D., Ortinau, L., Hoggatt, J., & Scadden, D. T. (2021). Chapter 4 - The skeletal stem cell. In D. W. Dempster, J. A. Cauley, M. L. Bouxsein, & F. Cosman (Eds.), *Marcus and Feldman's Osteoporosis* (5th ed., pp. 75–98). Academic Press.
Peng, W., Liu, Y.-J., Wu, N., Sun, T., He, X.-Y., Gao, Y.-X., & Wu, C.-J. (2015). Areca catechu L. (Arecaceae): A review of its traditional uses, botany, phytochemistry, pharmacology and toxicology. *Journal of Ethnopharmacology, 164*, 340–356. https://doi.org/10.1016/j.jep.2015.02.010.
Ruiz, M. B., Eguizábal, G. V., Villarreal, D. P., Busso, J. M., & López, A. G. (2019). Inhibitory action of thymol on fecal microbial activity in Tamandua tetradactyla and its effect on glucocorticoid metabolite measurement. *General and Comparative Endocrinology, 280*, 91–96. https://doi.org/10.1016/j.ygcen.2019.04.015.
Shi, H., Wang, B., Niu, L., Cao, M., Kang, W., Lian, K., & Zhang, P. (2017). Trace level determination of 5-hydroxytryptamine and its related indoles in amniotic fluid by gas chromatography–mass spectrometry. *Journal of Pharmaceutical and Biomedical Analysis, 143*, 176–182. https://doi.org/10.1016/j.jpba.2017.05.044.
Si, L., Shi, J., Gao, W., Zheng, M., Liu, L., Zhu, J., & Tian, J. (2014). Smad4 mediated BMP2 signal is essential for the regulation of GATA4 and Nkx2.5 by affecting the histone H3 acetylation in H9c2 cells. *Biochemical and Biophysical Research Communications, 450*(1), 81–86. https://doi.org/10.1016/j.bbrc.2014.05.068.
Song, Y., Shan, B., Li, H., Feng, B., Peng, H., Jin, C., … Su, D. (2019). Safety investigation of Pulsatilla chinensis saponins from chronic metabonomic study of serum biomedical changes in oral treated rat. *Journal of Ethnopharmacology, 235*, 435–445. https://doi.org/10.1016/j.jep.2019.01.035.
Southmayd, E. A., & De Souza, M. J. (2017). A summary of the influence of exogenous estrogen administration across the lifespan on the GH/IGF-1 axis and implications for bone health. *Growth Hormone & IGF Research, 32*, 2–13. https://doi.org/10.1016/j.ghir.2016.09.001.
Szmyd, B., Rogut, M., Białasiewicz, P., & Gabryelska, A. (2021). The impact of glucocorticoids and statins on sleep quality. *Sleep Medicine Reviews, 55*, Article 101380. https://doi.org/10.1016/j.smrv.2020.101380.
Tsukasaki, M., Asano, T., Muro, R., Huynh, N. C.-N., Komatsu, N., Okamoto, K., … Takayanagi, H. (2020). OPG production matters where it happened. *Cell Reports, 32*(10), Article 108124. https://doi.org/10.1016/j.celrep.2020.108124.
Wu, L., Li, L., Chen, S., Wang, L., & Lin, X. (2020). Deep eutectic solvent-based ultrasonic-assisted extraction of phenolic compounds from Moringa oleifera L. leaves: Optimization, comparison and antioxidant activity. *Separation and*

Purification Technology, 247, Article 117014. https://doi.org/10.1016/j.seppur.2020.117014.

Xia, G., Wang, J., Sun, S., Zhao, Y., Wang, Y., Yu, Z., … Xue, C. (2016). Sialoglycoproteins prepared from the eggs of Carassius auratus prevent bone loss by inhibiting the NF-κB pathway in ovariectomized rats [10.1039/C5FO00955C]. *Food & Function, 7*(2), 704–712. https://doi.org/10.1039/C5FO00955C.

Xia, T., Dong, X., Lin, L., Jiang, Y., Ma, X., Xin, H., … Qin, L. (2019). Metabolomics profiling provides valuable insights into the underlying mechanisms of Morinda officinalis on protecting glucocorticoid-induced osteoporosis. *Journal of Pharmaceutical and Biomedical Analysis, 166*, 336–346. https://doi.org/10.1016/j.jpba.2019.01.019.

Xiao, H. H., Sham, T. T., Chan, C. O., Li, M. H., Chen, X., Wu, Q. C., … Wong, M. S. (2018). A metabolomics study on the bone protective effects of a lignan-rich fraction from Sambucus Williamsii Ramulus in aged rats. *Frontiers in Pharmacology, 9*, 932. https://doi.org/10.3389/fphar.2018.00932.

Xu, F., Pandya, J. K., Chung, C., McClements, D. J., & Kinchla, A. J. (2018). Emulsions as delivery systems for gamma and delta tocotrienols: Formation, properties and simulated gastrointestinal fate. *Food Research International, 105*, 570–579. https://doi.org/10.1016/j.foodres.2017.11.033.

Yadav, V. K., Balaji, S., Suresh, P. S., Liu, X. S., Lu, X., Li, Z., … Ducy, P. (2010). Pharmacological inhibition of gut-derived serotonin synthesis is a potential bone anabolic treatment for osteoporosis. *Nature Medicine, 16*(3), 308–U103. https://doi.org/10.1038/nm.2098.

Yadav, V. K., Ryu, J. H., Suda, N., Tanaka, K. F., Gingrich, J. A., Schutz, G., … Karsenty, G. (2008). Lrp5 controls bone formation by inhibiting serotonin synthesis in the duodenum. *Cell, 135*(5), 825–837. https://doi.org/10.1016/j.cell.2008.09.059.

Yang, C., Huang, X., Wang, S., Han, M., Kang, F., Zhang, Z., & Li, J. (2020). Intrathecal administration of SRT1720 relieves bone cancer pain by inhibiting the CREB/CRTC1 signalling pathway. *Neuroscience Letters, 715*, Article 134623. https://doi.org/10.1016/j.neulet.2019.134623.

Yano, Jessica M., Yu, K., Donaldson, Gregory P., Shastri, Gauri G., Ann, P., Ma, L., … Hsiao, Elaine Y. (2015). Indigenous bacteria from the gut microbiota regulate host serotonin biosynthesis. *Cell, 161*(2), 264–276. https://doi.org/10.1016/j.cell.2015.02.047.

Yao, D., Huang, L., Ke, J., Zhang, M., Xiao, Q., & Zhu, X. (2020). Bone metabolism regulation: Implications for the treatment of bone diseases. *Biomedicine & Pharmacotherapy, 129*, Article 110494. https://doi.org/10.1016/j.biopha.2020.110494.

Yu, H., Lv, D., Shen, M., Zhang, Y., Zhou, D., Chen, Z., & Wang, C. (2019). BDNF mediates the protective effects of scopolamine in reserpine-induced depression-like behaviors via up-regulation of 5-HTT and TPH1. *Psychiatry Research, 271*, 328–334. https://doi.org/10.1016/j.psychres.2018.12.015.

Zhan, Q., Dai, Y., Wang, F., Mai, X., Fu, M., Wang, P., & Wang, J. (2019). Metabonomic analysis in investigating the anti-osteoporotic effect of sialoglycoprotein isolated from eggs of carassius auratus on ovariectomized mice. *Journal of Functional Foods, 61*. https://doi.org/10.1016/j.jff.2019.103514.

Zhang, M., Wang, Y., Zhang, Q., Wang, C., Zhang, D., Wan, J. B., & Yan, C. (2018). UPLC/Q-TOF-MS-based metabolomics study of the anti-osteoporosis effects of Achyranthes bidentata polysaccharides in ovariectomized rats. *International Journal of Biological Macromolecules, 112*, 433–441. https://doi.org/10.1016/j.ijbiomac.2018.01.204.

Zhang, R., Oyajobi, B. O., Harris, S. E., Chen, D., Tsao, C., Deng, H.-W., & Zhao, M. (2013). Wnt/β-catenin signaling activates bone morphogenetic protein 2 expression in osteoblasts. *Bone, 52*(1), 145–156. https://doi.org/10.1016/j.bone.2012.09.029.

Zhao, H.-J., Chang, H.-M., Klausen, C., Zhu, H., Li, Y., & Leung, P. C. K. (2020). Bone morphogenetic protein 2 induces the activation of WNT/β-catenin signaling and human trophoblast invasion through up-regulating BAMBI. *Cellular Signalling, 67*, Article 109489. https://doi.org/10.1016/j.cellsig.2019.109489.

Zhong, X. H., Lu, Q., Zhang, Q., He, Y., Wei, W. J., & Wang, Y. M. (2020). Oral microbiota alteration associated with oral cancer and areca chewing. *Oral Diseases*. https://doi.org/10.1111/odi.13545.

Zhu, H., Zhang, J., Li, C., Liu, S., & Wang, L. (2020). Morinda citrifolia L. leaves extracts obtained by traditional and eco-friendly extraction solvents: Relation between phenolic compositions and biological properties by multivariate analysis. *Industrial Crops and Products, 153*, Article 112586. https://doi.org/10.1016/j.indcrop.2020.112586.